Dasatinib (BMS-354825) Tyrosine Kinase Inhibitor Suppresses Invasion and Induces Cell Cycle Arrest and Apoptosis of Head and Neck Squamous Cell Carcinoma and Non–Small Cell Lung Cancer Cells

Faye M. Johnson,[1] Babita Saigal,[2] Moshe Talpaz,[2] and Nicholas J. Donato[2,3]

Abstract

Purpose: Epithelial tumors, including non–small cell lung cancer (NSCLC) and head and neck squamous cell carcinoma (HNSCC), present clinical challenges. One potential target for systemic therapy is Src family nonreceptor tyrosine kinases, which are overexpressed in these tumors and induce pleiotropic effects, including increased proliferation, enhanced survival, stimulation of angiogenesis, and changes in motility. Dasatinib (BMS-354825), an ATP-competitive, small molecule tyrosine kinase inhibitor, suppresses the activity of these kinases at subnanomolar concentrations. Therefore, we tested the antitumor effects of this inhibitor *in vitro* to determine whether *in vivo* analyses were warranted.

Experimental Design: The antitumor effects of dasatinib on HNSCC and NSCLC cells were evaluated using assays to measure cell cycle progression, apoptosis, migration, and invasion. Western blotting was used to monitor its effects on cell signaling.

Results: Dasatinib inhibited migration and invasion in all cell lines and induced cell cycle arrest (blocking the G_1-S transition) and apoptosis in some lines. The effects on migration and invasion correlated with the inhibition of Src and downstream mediators of adhesion [e.g., focal adhesion kinase (FAK), p130, and paxillin], and the cell cycle effects and apoptosis correlated with the induction of p27 and the dephosphorylation of Rb. Dasatinib also induced morphologic changes that were consistent with an upstream role for Src in regulating focal adhesion complexes.

Conclusions: This study showed that Src inhibition in HNSCC and NSCLC has antitumor effects *in vitro*. This suggests that dasatinib would have therapeutic activity against these tumors. Clinical studies in these tumor types are warranted.

Epithelial cancers, particularly lung cancer and head and neck squamous cell carcinoma (HNSCC), continue to pose formidable challenges in clinical practice. Novel chemotherapeutic agents have been developed, but even those have limited long-term benefits in the treatment of these tumors, illustrating the need to continue to improve systemic therapy for affected patients.

One promising target in this effort is found in the Src family of nonreceptor tyrosine kinases. Src regulates signals from multiple cell surface molecules, including integrins, growth factors, and G protein–coupled receptors. Although Src has been extensively studied, its exact role in the physiology of normal and malignant cells is complex and not completely understood (1). The activation of one family member, c-Src, is known to have pleiotropic effects that depend on the cell type and context. In malignant cells, c-Src activation can mediate transformation, proliferation, survival, angiogenesis, and motility (2–4).

In epithelial tumors, c-Src is overexpressed and activated, and the levels of expression or activation generally correlate with disease progression (3), although activating mutations are rare (5). In contrast, reduced c-Src expression in colon cancer cells suppresses tumor growth and blocks the expression of vascular endothelial growth factor (6–8). Although c-Src does promote the malignant phenotype in several tumor types, little is known about the consequences of inhibiting it in aerodigestive tumors because few studies have investigated its role in such epithelial cancers. Studies have shown that c-Src is activated in non–small cell lung cancer (NSCLC) tumor tissues from patients (9, 10), and its inhibition did lead to decreased anchorage-dependent cell growth and to cell cycle arrest and apoptosis (11, 12). In HNSCC tumor tissue from patients, c-Src is also overexpressed (13, 14) and other Src-related kinases (e.g., Yes, Fyn, and Lyn) are also present and signal through the activation of signal transducers and activators of transcription 3 (STAT3)

Authors' Affiliations: [1]Thoracic/Head and Neck Medical Oncology and [2]Experimental Therapeutics, University of Texas M.D. Anderson Cancer Center and [3]Program in Cancer Biology, University of Texas Graduate School of Biomedical Sciences at Houston, Houston, Texas

Received 4/5/05; revised 6/6/05; accepted 7/7/05.

Grant support: Physician Scientist Award from M.D. Anderson Cancer Center (F.M. Johnson) and grant PO1 CA46939 (N.J. Donato).

The costs of publication of this article were defrayed in part by the payment of page charges. This article must therefore be hereby marked *advertisement* in accordance with 18 U.S.C. Section 1734 solely to indicate this fact.

Requests for reprints: Faye M. Johnson, Department of Thoracic/Head and Neck Medical Oncology, Unit 432, University of Texas M.D. Anderson Cancer Center, 1515 Holcombe Boulevard, Houston, TX 77030-4009. Phone: 713-792-6363; Fax: 713-796-8655; E-mail: fmjohns@mdanderson.org.

doi:10.1158/1078-0432.CCR-05-0757

and STAT5 (15). As expected, inhibiting the Src family kinases in HNSCC cell lines led to decreased growth *in vitro* (15).

One agent that could prove useful in the clinical application of this knowledge is dasatinib (BMS-354825), an ATP-competitive tyrosine kinase inhibitor that sensitively inhibits all members of the Src family, including c-Src, Lck, Fyn, and Yes (IC_{50} < 1.1 nmol/L; refs. 16–18). At higher concentrations (3 to 28 nmol/L), dasatinib also inhibits the Src kinases Abl, c-Kit, PDGFR, and EphA2 (16). To evaluate the potential of dasatinib in the treatment of HNSCC and NSCLC, we used a variety of assays to measure its effects on cell cycle progression, apoptosis, migration, and invasion. Our studies suggest that this inhibitor potently suppresses c-Src activation and induces multiple antitumor effects in aerodigestive tumor cells, making it a candidate for *in vivo* tests of its effectiveness.

Materials and Methods

Materials. Dasatinib was provided by Bristol-Myers Squibb (New York, NY) and was prepared as a 10 mmol/L stock solution in DMSO. Antibodies used in Western blotting included mitogen-activated protein kinase (MAPK) and phosphorylated MAPK (Promega, Madison, WI); AKT and phosphorylated AKT (New England Biolabs, Beverly, MA); Src (Santa Cruz Biotechnology, Santa Cruz, CA); pY418-c-Src, p27, Rb, phospho-Rb, pY705-STAT3, pY249-p130Cas, pY694-STAT5, pY925-FAK, and pY576-FAK (Cell Signaling Technology, Beverly, MA); pY861-FAK (Biosource, Camarillo, CA); FAK, pTyrosine, and EphA2 (Upstate Biotechnology, Lake Placid, NY); paxillin (Zymed Laboratories, South San Francisco, CA); and actin (Sigma Chemical Company, St. Louis, MO). Matrigel, Annexin V, and collagen I– and laminin-coated cell culture plates were obtained from BD Biosciences (San Diego, CA).

Cell culture. Twelve human cancer cell lines were used in this study: eight HNSCC cell lines (obtained from Dr. J. Myers and Dr. G. Clayman of University of Texas M. D. Anderson Cancer Center) and four NSCLC cell lines (obtained from American Type Culture Collection, Manassas, VA; Table 1). Cells were grown in monolayer cultures in DMEM (HNSCC cells) or RPMI 1640 (NSCLC cells) containing 10% fetal bovine serum and 2 mmol/L glutamine at 37°C in a humidified atmosphere of 95% air and 5% CO_2. Crystal violet staining was used to gauge the effects of dasatinib on the growth and adhesion of all cell lines, as previously described (19). Preliminary studies showed that DMSO (≤0.2% was the maximal amount used to deliver dasatinib) had no effect on cell viability, cell cycle, apoptosis, or signaling (data not shown). Conditioned medium was obtained from 3T3 cells grown in DMEM.

Crystal violet staining. To assess the effect of dasatinib on cell numbers, we plated cells into 96-well plates and incubated them for 24 hours using the conditions described above for standard cell culture maintenance. The cells were subsequently exposed to dasatinib at various concentrations for 72 hours. Four or more wells were treated at each concentration. Medium was removed from the 96-well plates and adherent cells were fixed and stained with crystal violet (0.5% crystal violet and 20% methanol) for 30 minutes. The plates were washed with distilled water and the stain was extracted with Sorenson's buffer [0.1 mol/L sodium citrate (pH 4.2) and 50% ethanol] overnight at 4°C (20). The absorbance of individual wells was read at 570 nm. The results are reported as the ratio of the average absorbance value from treated cells to the average control value from four or more replicates.

Trypan blue exclusion. Subconfluent cells were treated with 0 to 10 μmol/L dasatinib for 72 hours. After treatment, cells were harvested with trypsin, stained with trypan blue, and counted manually with a hemacytometer. Cells that excluded trypan blue were considered viable.

Cell cycle analysis. Subconfluent cells were treated with 100 nmol/L dasatinib for 24 to 48 hours. Cells were harvested, washed in PBS, fixed in 1% paraformaldehyde, rewashed in PBS, and resuspended in 70% ethanol at −20°C overnight. Cells were washed twice with PBS and stained with 20 μg/mL propidium iodide. DNA content was analyzed on a cytofluorimeter by fluorescence-activated cell sorting analysis (FACScan, Becton Dickinson and Company, San Jose, CA) using ModFit software (Verity Software House, Turramurra, NSW, Australia).

Apoptosis assay. Subconfluent cells were treated with 100 nmol/L dasatinib for 24 hours. Cells were then harvested and stained with Annexin V and propidium iodide and analyzed on a cytofluorimeter by FACScan using ModFit software.

Morphology. HNSCC or NSCLC cells were plated directly onto laminin- or collagen I–coated wells. After 24 hours, 100 nmol/L dasatinib was added, and serial photographs were taken after 15 minutes, 4 hours, and 24 hours.

Migration assay (scratch assay). HNSCC and NSCLC cells were grown to confluence on tissue culture dishes and a single scrape was made in the confluent monolayer using a sterile pipette tip. The monolayer was washed with PBS and complete medium containing 100 nmol/L dasatinib or DMSO alone was added. Serial photographs of the same scraped section were taken every 6 hours for 72 hours (21). The number of cells that had migrated over the margins of the wounds was counted after 6 hours (12 hours for H322 cells; ref. 22). The time required for the scrape to close was also recorded.

Table 1. Head and neck squamous cell carcinoma and NSCLC cell lines and their dasatinib IC_{50}

Cell line	Cell type	Genetic background	IC_{50} (nmol/L)
686LN	HNSCC, lymph node, base tongue primary	Wt *p53*	30
Tu167	HNSCC, floor of mouth primary	Mutant *p53*	50
MDA1986	HNSCC, lymph node, base tongue primary	Wt *p53*	60
Tu159	HNSCC, tongue primary	ND	90
JMAR	HNSCC, anoikis-resistant Tu167	Mutant *p53*	250
Tu686	HNSCC, base tongue primary	Mutant *p53*	540
LN158	HNSCC, lymph node from tonsil primary	ND	1,600
358B	HNSCC, buccal mucosal tumor	ND	2,100
H322	NSCLC, adenocarcinoma	Mutant *p53,* wt K-*ras*, wt EGFR	80
H460	NSCLC, large cell	Wt *p53,* wt K-*ras*, wt EGFR	1,800
H226	NSCLC, squamous cell	Mutant *p53,* wt K-*ras*, wt EGFR	10,000
A549	NSCLC, adenocarcinoma	Wt *p53,* mutant K-*ras*, wt EGFR	10,000

Abbreviations: ND, not determined; wt, wild type.

Invasion assay. The invasive capacity of HNSCC and NSCLC cells was measured using a modified Boyden chamber (23). The chambers consist of a porous filter (with pores 8 μm in diameter) that separates the chamber into two compartments. The top of each filter is coated with Matrigel. Cells to be assayed were placed into the upper compartment in complete medium, and serum-free medium was placed in the lower compartment; the cells were allowed to attach and spread for 16 hours. Then, 10 nmol/L (for HNSCC) or 50 nmol/L (for NSCLC) dasatinib were added to the cells, and 3T3 conditioned medium (as a chemoattractant) was placed into the bottom compartment. After 24 hours of incubation under standard tissue culture conditions, cells on the top of the filter (those that had not invaded through the filter) were scraped off and discarded. The remaining cells (i.e., those that had invaded through the Matrigel and the filter) were fixed, stained, and counted by light microscopy. In parallel, cells from the same lines were treated identically in 24-well plates. These cells were harvested, stained with trypan blue, and counted. The number of cells that had invaded was normalized for effects on cell viability.

Western blot. Detached cells from each cell culture plate were collected by centrifugation, washed in PBS, and added to the cell lysate from their corresponding plates. Adherent cells were rinsed with ice-cold PBS and lysed in the cell culture plate for 20 minutes on ice in lysis buffer consisting of 50 mmol/L Trizma base (pH 8; Sigma), 1% Triton X-100, 150 mmol/L NaCl, 20 μg/mL leupeptin, 10 μg/mL aprotinin, 1 mmol/L phenylmethylsulfonyl fluoride, and 1 mmol/L sodium vanadate. Lysates were spun in a centrifuge at 14,000 rpm for 5 minutes and the supernatant was collected. Equal protein aliquots were resolved by SDS-PAGE, transferred to nitrocellulose membranes, immunoblotted with primary antibody, and detected with horseradish peroxidase–conjugated secondary antibody (Bio-Rad Laboratories, Hercules, CA) and enhanced chemiluminescence reagent (Amersham Biosciences, Piscataway, NJ).

Immunoprecipitation. Cells were lysed as described for Western blotting. Equal amounts of protein cell lysates (200-300 μg in lysis buffer) were precleared with Protein G Sepharose beads (Sigma-Aldrich, St. Louis, MO) for 1 hour. The precleared lysate was incubated with 5 μg of anti-FAK or paxillin antibody for 2 hours and then incubated with 30 μL of the beads for 1 hour. The beads were washed four times with immunocomplex buffer [0.5% Triton X-100, 0.5% NP40, 150 mmol/L NaCl, 10 mmol/L Tris (pH 7.4), 1 mmol/L EDTA, 1 mmol/L EGTA, 1 mmol/L sodium vanadate, 1 mmol/L phenylmethylsulfonyl fluoride] and resolved by SDS-PAGE. Resolved precipitate was blotted with the indicated antibody, which was detected with secondary antibody and enhanced chemiluminescence reagent. Then, the membrane was stripped, reprobed with anti-FAK or paxillin antibody (loading control), and detected with secondary antibody and enhanced chemiluminescence reagent.

Results

Src inhibition by dasatinib inhibits cell growth in head and neck squamous cell carcinoma and non–small cell lung cancer cell lines. All 12 cell lines were tested for sensitivity to dasatinib *in vitro* using a crystal violet assay. The IC_{50}, after treatment in complete medium for 72 hours, was calculated (Table 1). In general, the HNSCC cell lines were markedly more sensitive than the NSCLC cell lines with the exception of H322. Serum levels of up to 2 μmol/L have been detected in patients with leukemia treated with dasatinib in a phase I trial without significant toxicity (24, 25). Cell lines were also tested for sensitivity using the trypan blue exclusion assay under the same conditions. Cell lines were shown to be either equally or more sensitive to dasatinib by trypan blue exclusion than by crystal violet staining. Representative data are shown in Fig. 1. Inhibition of cell growth was shown to be dose dependent

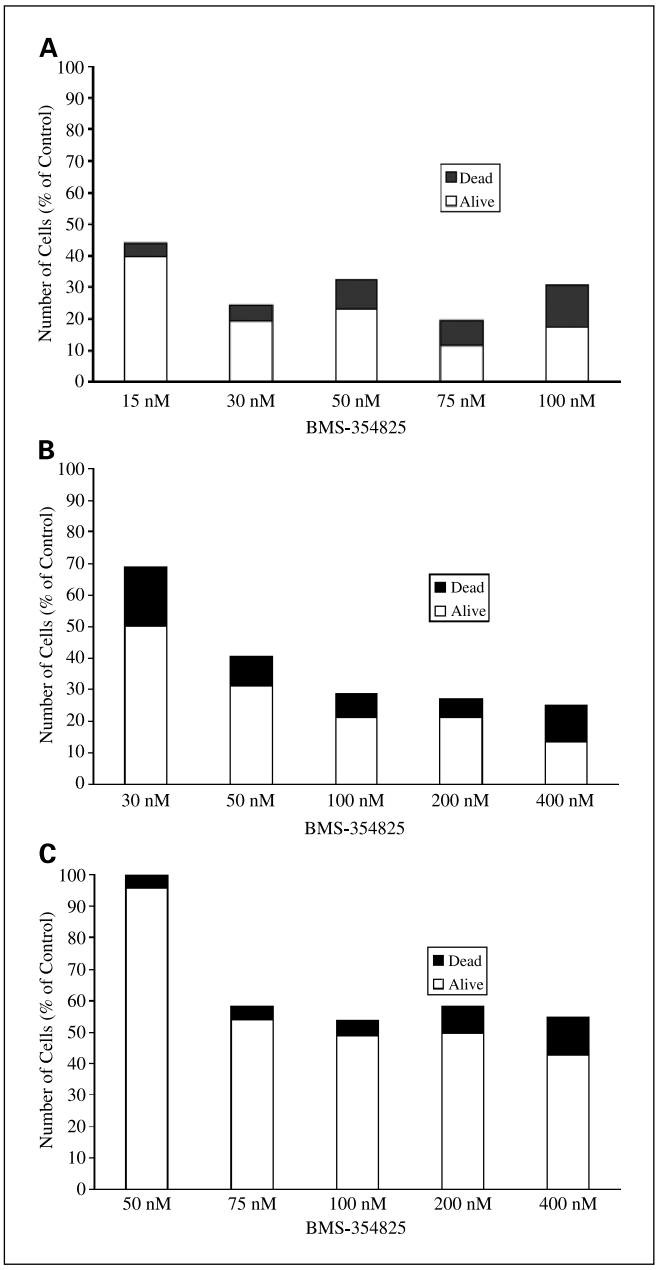

Fig. 1. Representative cytotoxicity using trypan blue exclusion after treatment with BMS-354825 for 72 hours at the given concentrations in Tu167 (*A*), JMAR (*B*), and H322 (*C*) cells *in vitro*. *Columns,* percentage of control cells (treated with DMSO alone) with cells that excluded trypan blue (alive) in white and cells that stained with trypan blue (dead) in black.

by both assays, although a plateau of inhibition was reached for all cell lines (Fig. 1). For any cell line with an IC_{50} below 100 nmol/L, complete inhibition of cell growth and survival was observed at concentrations >500 nmol/L (data not shown).

HNSCC cells (Tu167 and JMAR) and NSCLC cells (A549 and H322) were treated with 100 nmol/L dasatinib in complete medium for 24 to 48 hours, and cell cycle progression was analyzed by fluorescence-activated cell sorting analysis (Fig. 2). JMAR, Tu167, and H322 cells treated with dasatinib showed a decreased percentage of cells in G_2-M and S phases and an increased number of cells in the sub-G_0 population, consistent with cell cycle blockage in the

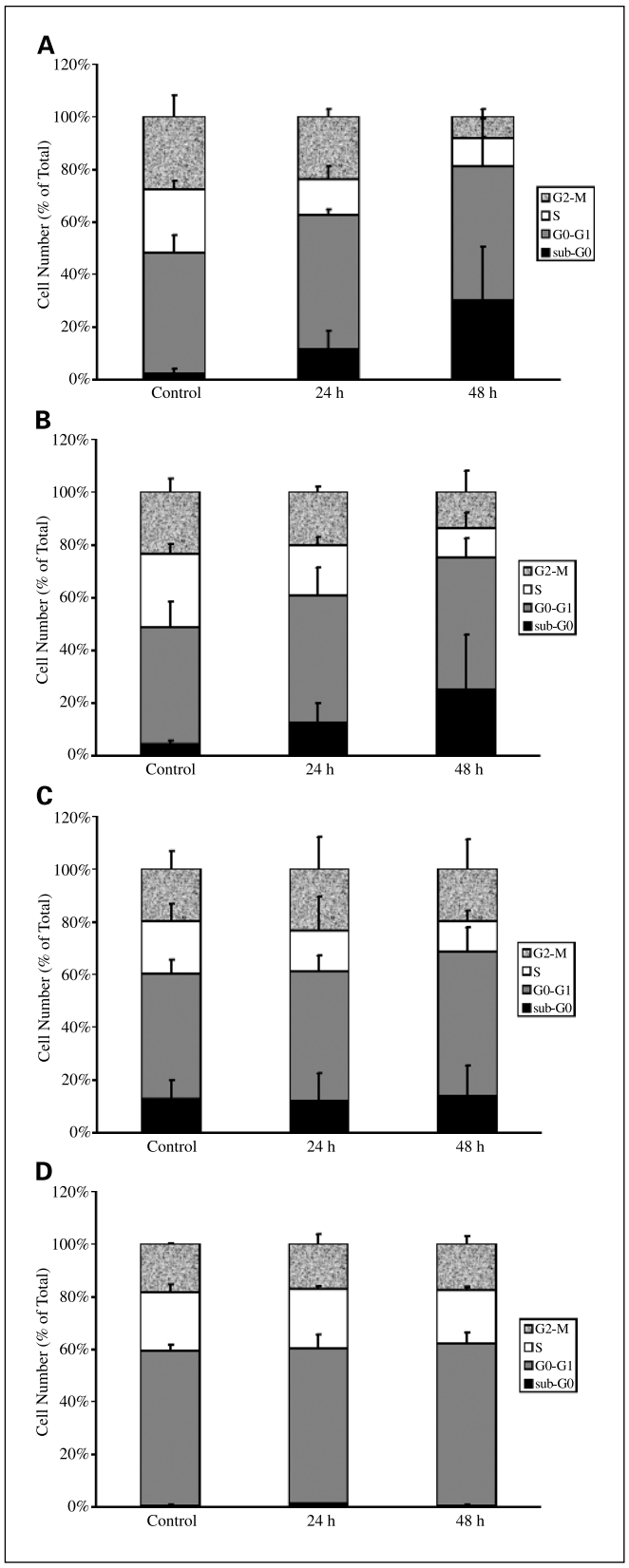

Fig. 2. Effect of BMS-354825 on the cell cycle. Cells (*A,* Tu167; *B,* JMAR; *C,* H322; *D,* A549) were treated for 0, 24, or 48 hours with 100 nmol/L BMS-354825, fixed, stained with propidium iodide, and analyzed by FACScan. Three separate experiments were done and combined. *Bars,* SD. There was no significant effect on control cells grown in parallel (data not shown).

G_1-to-S transition and induction of apoptosis. This was in contrast to markedly insensitive cells (A549, IC_{50} = 10,000 nmol/L) in which dasatinib had no effect on cell cycle progression (Fig. 2D) even when the cells were treated with 500 nmol/L dasatinib (data not shown).

Src inhibition leads to apoptosis. HNSCC cells (Tu167 and JMAR) and NSCLC cells (A549 and H322) were treated with 100 nmol/L dasatinib in complete medium for 24 hours. Cells were stained with both propidium iodide and Annexin V and analyzed by fluorescence-activated cell sorting analysis (Fig. 3). Only 20% of the Tu167 cells remained alive and Annexin V negative after treatment. Moderate levels of apoptosis were detected in H322 and JMAR cells, but A549 cells were unaffected. These results are consistent with the crystal violet, trypan blue, and cell cycle analyses presented above.

Src inhibition leads to substrate-dependent cell morphology changes. Integrins mediate diverse interactions between cells and the intracellular matrix. Laminin and collagen receptor integrins are distinct, both structurally and biologically (26, 27). Sensitive HNSCC and NSCLC cells were plated in complete medium onto tissue culture plates coated with either collagen I or laminin. After 24 hours, 100 nmol/L dasatinib was added and serial photographs were taken (Fig. 4). Cells plated on laminin showed signs of detachment within 5 minutes of treatment with dasatinib and nearly all of the cells were detached or loosely attached to the culture plate after 24 hours. In contrast, there was no discernable immediate change in morphology in dasatinib-treated or control cells plated on collagen I. Decreased cell spreading was observed after 24 hours of treatment.

Src inhibition causes decreased migration and invasion. All eight cell lines were treated with 100 nmol/L dasatinib and cell migration was measured using the scratch assay described above. The number of cells that had migrated into the scratch after 6 hours was calculated and is shown in Fig. 5. Cell number was not significantly affected after 6 hours of treatment with 100 nmol/L dasatinib (data not shown). Cells from three of the NSCLC lines (A549, H460, and H226) did not migrate in this assay even in the untreated control samples. H322 cells migrated more slowly than the HNSCC cell lines, and the number of cells that had migrated after 12 hours was thus used to gauge the effect of treatment. The kinetics of cell migration in the wound and the closure of the wound were also noted. There was no significant wound closure after 72 hours in any of the treated cell lines, but there was complete wound closure in 24 to 36 hours in all of the untreated cell lines (HNSCC and H322).

Cell invasion was measured using a modified Boyden chamber with a Matrigel-coated filter (Fig. 6). In this assay, longer times were needed and drug concentrations were reduced to minimize the effects of dasatinib on cell viability. Cell migration and invasion were significantly inhibited by dasatinib, regardless of the antiproliferative or apoptotic response of the cells to the drug.

Dasatinib inhibits Src activity and downstream signaling. The effects of dasatinib on cell signaling were evaluated in four HNSCC and four NSCLC cell lines with wide diversity in their antiproliferative or apoptotic sensitivity to dasatinib. The baseline levels of Src and activated Src (pY418-Src) were measured by Western blotting (Fig 7A). There was no consistent correlation between the expression or activation of Src at

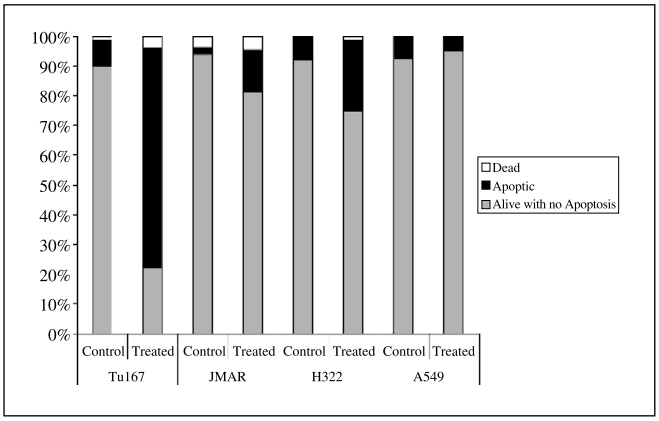

Fig. 3. Effect of BMS-354825 on apoptosis. Cells were treated for 24 hours with 100 nmol/L BMS-354825, stained with Annexin V and propidium iodide, and analyzed by FACScan. Cells were then classified as alive with no apoptosis (i.e., propidium iodide negative, Annexin V negative), dead (i.e., propidium iodide positive), or apoptotic (i.e., Annexin V positive).

baseline and the biological effects of dasatinib in these cell lines. Dasatinib caused complete or near-complete inhibition of Src activity, as measured by phosphorylation at Y418 in Western blotting after treatment for 15 minutes with concentrations of 100 nmol/L or higher in all eight cell lines (representative data; Fig. 7B).

The effects of 100 nmol/L dasatinib on Src and known downstream targets were examined by Western blotting in cells treated for 2 to 24 hours (Fig. 8). Again, we found that Src activity was significantly inhibited in all cell lines, but total Src levels were not affected. In all cell lines, FAK phosphorylation was decreased at the Src-dependent sites (Y576/577, Y861, and Y925) and, as predicted, unaffected at Y397 (Fig. 8A-C). Complete inhibition of paxilllin and p130Cas phosphorylation was also observed in all cell lines. In HNSCC cells, MAPK activity was transiently decreased in HNSCC cells and was affected in only one sensitive NSCLC cell line (H322). STAT5 activation was reduced in all cell lines, and STAT3 activation was transiently reduced and returned to baseline levels within 24 hours. When HNSCC cells were treated at higher doses (500 nmol/L), STAT3 was activated by dasatinib (Fig. 8D). Inhibition of AKT phosphorylation was variable, and, in general, there was more inhibition in sensitive cell lines. A more striking correlation was found between the antiproliferative effects of dasatinib and the modulation of p27 expression. Levels of p27 were up-regulated by dasatinib in H322 but not in the other NSCLC cell lines. In HNSCC, more marked effects on p27 were seen in the more sensitive cell

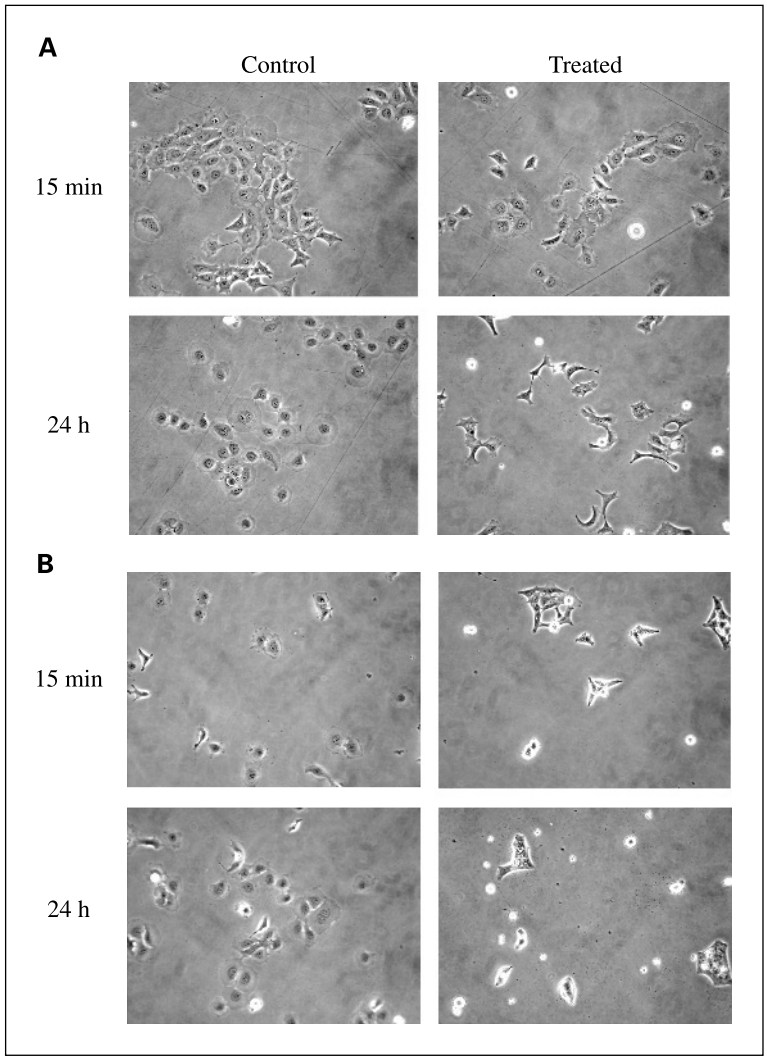

Fig. 4. Effect of BMS-354825 on cell morphology. Tu167 cells were plated on either collagen I (*A*) or laminin (*B*) for 24 hours and then treated with 100 nmol/L BMS-354825 for 24 hours. Serial photographs were taken, and representative fields are shown.

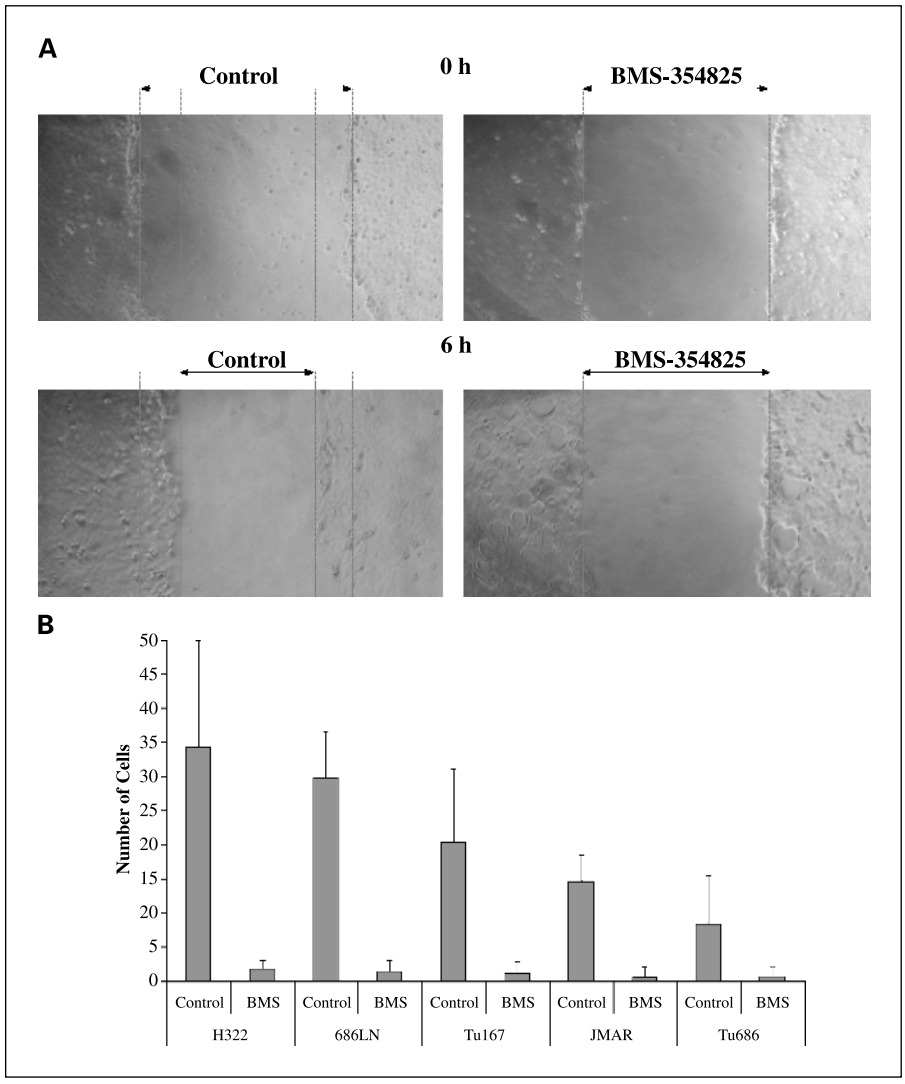

Fig. 5. Effect of BMS-354825 on cell migration. Cells were plated to confluence on tissue culture plastic. A single scratch was made in the confluent monolayer. The scratch was monitored and photographed every 6 hours (representative data, *A*). Cells that migrated into the scratch after 6 hours (12 hours for H322) were counted (*B*). The data represent four independent experiments; bars, SD. In all cases, when treated samples are compared with corresponding controls, $P < 0.05$.

lines. A similar correlation was seen between cell cycle effects (Fig. 2) and levels of pRb and total Rb after treatment. The induction of p27 after dasatinib treatment correlated with the loss of Rb phosphorylation. In one cell line (Tu686), an apparent loss of total Rb was also observed.

Discussion

This study showed that clinically achievable levels of dasatinib led to cell cycle arrest and apoptosis in some HNSCC and NSCLC cell lines. Cells lines with high sensitivity (low IC_{50} values), as measured by crystal violet and trypan blue exclusion analyses, showed cell cycle arrest and significant apoptosis. However, in all cell lines, low doses of dasatinib (≤100 nmol/L) inhibited cell migration and invasion independent of any effects on cell proliferation and survival.

Src expression and inhibition did not predict changes in cell cycle arrest, apoptosis, or growth inhibition in response to dasatinib in these cell lines. However, changes in the phosphorylation of specific downstream signaling proteins by dasatinib did seem to correlate with proliferation and survival. In one sensitive NSCLC cell line (H322, IC_{50} = 80 nmol/L) and all HNSCC cell lines (IC_{50} = 30-540 nmol/L), there was an induction of p27 and a reduction of pRb; in contrast, there was no effect on p27 or Rb in the remaining NSCLC cell lines (IC_{50} = 1,800 to 10,000 nmol/L). This correlation was consistent with the roles of Rb and p27 in regulating cell cycle progression and survival (28). We also examined the Ras-MAPK pathway because it is affected by Src, possibly via its interactions with Shc (29, 30). Src also regulates FAK activation and is directly linked to the Ras-MAPK pathway through growth factor receptor binding protein 2 recruitment to FAK via tyrosine phosphorylation. In addition, cell cycle regulation by dasatinib may be mediated through MAPK activation and changes in p27 phosphorylation. Inhibition of Src by dasatinib led to a delayed reduction in MAPK activation and, in some cell lines, a transient reactivation of this pathway was observed. These results show that inhibition of Src does not have sustained effects on the MAPK cascade in head and neck tumors and other compensatory signals may be involved in the observed effects of dasatinib on MAPK regulation.

The diversity of biological and molecular responses to dasatinib was not unexpected. For example, epidermal growth factor receptor (EGFR) inhibitors also show diverse biological and molecular effects in patient tumors and cell lines that are

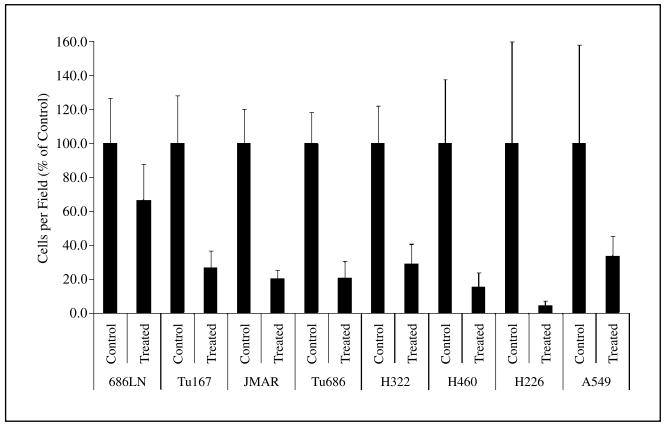

Fig. 6. Effect of BMS-354825 on cell invasion. Cells were plated onto Matrigel-coated filters in a modified Boyden chamber. Cells were allowed to attach and spread for 16 hours before the addition of 10 nmol/L (for HNSCC cells) or 50 nmol/L (for NSCLC cells) BMS-354825 to the upper chamber and conditioned medium to the lower chamber. After 24 hours, cells still in the upper chamber were removed and cells that had invaded through the Matrigel were stained and counted. In parallel, cells treated identically were assessed for viability and cell number with trypan blue. The average number of cells per field is expressed as a percentage of the control after normalizing for cell number. The concentration of BMS-354825 was lowered in this experiment to minimize its effect on the absolute cell number. In all cases, when treated samples are compared with corresponding controls, $P < 0.05$.

independent of the degree of EGFR expression (31, 32). Although some of this may be due to EGFR mutation, an uncoupling of EGFR inhibition from downstream biological effects is also seen in many cell lines (32–35). There were no known genetic mutations that influenced cell sensitivity to dasatinib (Table 1). Inactivating p53 mutations are found commonly in both NSCLC and HNSCC. In addition, activating Ras mutations (predominantly K-*ras*) and EGFR mutations are also found in NSCLC. We did not find any relationship between

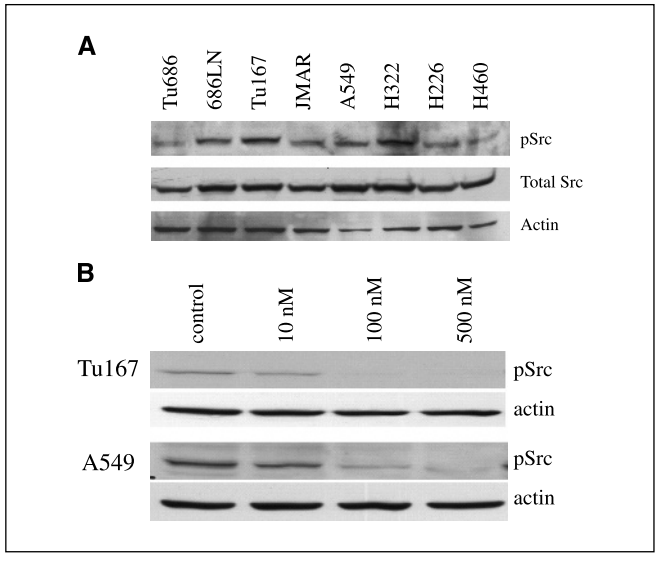

Fig. 7. Baseline Src expression and inhibition by BMS-354825. Western blot analysis of untreated cells revealed that all cell lines expressed Src and activated Src (*A*). A dose-response effect of BMS-354825 on Src activation was observed in all cell lines by Western blot after treatment for 15 minutes. Src activation was inhibited partially by 10 nmol/L BMS-354825 and maximally at doses >100 nmol/L (two representative cell lines, *B*).

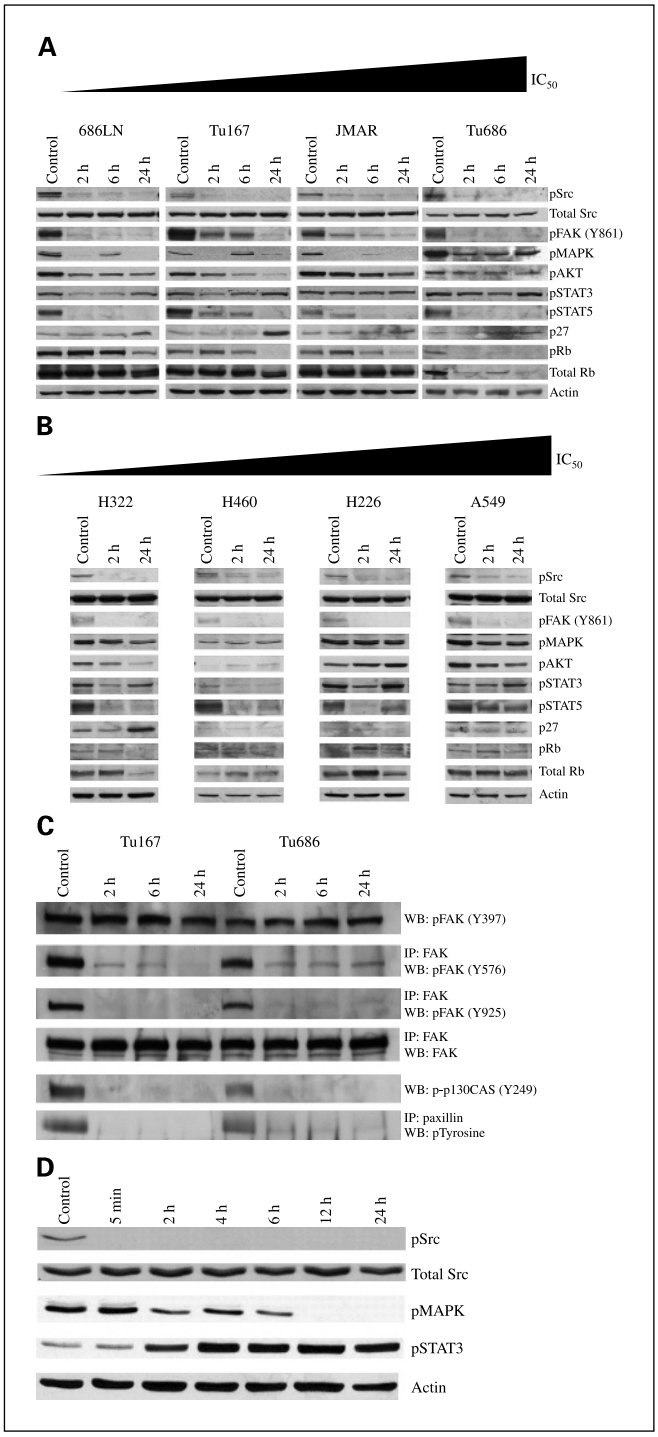

Fig. 8. The effect of BMS-354825 on cell signaling. Cells were treated with 100 nmol/L (*A*, *B*, and *D*) or 500 nmol/L (*C*) BMS-354825 for the indicated times, lysed, and analyzed by Western blotting (*WB*) or immunoprecipitation (*IP*) with the indicated antibodies. Cell lines are as indicated; Tu167 cells were used in (*D*).

p53 or K-*ras* mutation status and sensitivity to dasatinib. None of our cell lines had EGFR mutations, but these cell lines may be more sensitive to Src inhibition (36).

In contrast, dasatinib inhibited cell migration and invasion in all cell lines tested, regardless of the effects seen on proliferation and survival. This is consistent with the defined role of Src in the

migration and attachment of epithelial cells. Src is part of the focal adhesion complex that links integrins to the cytoskeleton. Here, along with FAK and other proteins, it promotes cell motility by turnover of the focal adhesion. Src inactivation by c-Src tyrosine kinase is associated with stabilization of this complex and reduced cell motility and invasion (37). In addition, Src activation is associated with reduced cell-to-cell adhesion via disruption of the adherins junction, which is needed for cell motility and invasion. A role for integrins is suggested by the morphologic changes induced by dasatinib on laminin that were not observed on collagen I matrices. The functional cellular receptor for collagen I is $\alpha_2\beta_1$ integrin (26), whereas numerous integrins recognize laminin (38). Although FAK and Src activation are central to most integrin signaling, β_1 integrins can signal independently of FAK and Src (39).

Like all pharmacologic agents, dasatinib is not completely specific, and it seems that not all of its biological and molecular effects are due to Src inhibition. Although dasatinib also inhibits c-kit, Abl, and PDGFR, we believe that it is unlikely that dasatinib mediates a significant effect on cell cycle progression or apoptosis, because such effects were not seen in these same cells lines treated with imatinib at doses in excess of those needed to inhibit these kinases (5 μmol/L; refs. 40, 41). Another possible therapeutic target is EphA2, the expression of which correlates with an advanced stage and poor prognosis in NSCLC (42). In a separate study of all of the cell lines used in these studies, EphA2 was expressed, and phosphorylation of EphA2 was rapidly reduced (within 15 minutes) by 100 nmol/L dasatinib. However, there was no correlation between the effects of the drug on EphA2 phosphorylation and its effects on cell cycle progression and apoptosis.[4] In two of the NSCLC cell lines, the IC_{50} of dasatinib was 10,000 nmol/L. The molecular mechanism for the effects of dasatinib on cell viability at this concentration are not due to Src inhibition alone but may be associated with the nonspecific effects of dasatinib on multiple kinases or other targets that can occur at high concentration (16).

The lack of long-term STAT3 inhibition and the activation of STAT3 at higher doses was unexpected. STAT3 inhibition did not follow the durable inhibition of c-Src after incubation with dasatinib. This was not predicted by previous studies, which suggested that STAT3 is downstream of Src and is responsible for some of its many biological functions, such as angiogenesis (12, 15, 43). The activation of STAT3 may be a compensatory effect that suppresses the proapoptotic or antiproliferative effects of dasatinib. Combining STAT3 inhibitors with dasatinib in HNSCC and NSCLC may lead to additive or synergistic antitumor effects. This is currently being examined.

Further study of dasatinib in HNSCC and NSCLC is warranted on the basis of these results. The universal effects seen on migration and invasion suggest that beneficial clinical effects may be achieved without direct cancer cell cytotoxicity. In addition, on the basis of previous studies, we would expect Src inhibition to affect angiogenesis (43). These effects may be detected in animal models of HNSCC and NSCLC.

This study has revealed the biological and kinase inhibitory effects of the potent c-Src inhibitor dasatinib on tumor cells derived from the aerodigestive tract. This drug is currently being examined in patients with chronic myelogenous leukemia who have failed imatinib-based therapy (24, 25). The early results provided here suggest that this agent may also have antitumor activity in other cancers. The apoptotic effects of dasatinib in HNSCC cells parallel those observed in chronic myelogenous leukemia cells and suggest that clinical trials in patients with HNSCC may reveal a subset of patients who benefit from this form of target-specific inhibition. In addition, the universal effect of dasatinib on cell migration and invasion in HNSCC and NSCLC cell lines suggest that an *in vivo* antitumor effect may be more extensive than predicted by direct cytotoxic effects.

[4] Unpublished data.

References

1. Yeatman TJ. A renaissance for SRC. Nat Rev Cancer 2004;4:470–80.
2. Frame MC. Src in cancer: deregulation and consequences for cell behaviour. Biochim Biophys Acta 2002;1602:114–30.
3. Irby RB, Yeatman TJ. Role of Src expression and activation in human cancer. Oncogene 2000;19:5636–42.
4. Schlessinger J. New roles for Src kinases in control of cell survival and angiogenesis. Cell 2000;100:293–6.
5. Irby RB, Mao W, Coppola D, et al. Activating SRC mutation in a subset of advanced human colon cancers. Nat Genet 1999;21:187–90.
6. Fleming RY, Ellis LM, Parikh NU, Liu W, Staley CA, Gallick GE. Regulation of vascular endothelial growth factor expression in human colon carcinoma cells by activity of src kinase. Surgery 1997;122:501–7.
7. Ellis LM, Staley CA, Liu W, et al. Down-regulation of vascular endothelial growth factor in a human colon carcinoma cell line transfected with an antisense expression vector specific for c-src. J Biol Chem 1998;273:1052–7.
8. Staley CA, Parikh NU, Gallick GE. Decreased tumorigenicity of a human colon adenocarcinoma cell line by an antisense expression vector specific for c-Src. Cell Growth Differ 1997;8:269–74.
9. Masaki T, Igarashi K, Tokuda M, et al. pp60(c-src) activation in lung adenocarcinoma. Eur J Cancer 2003;39:1447–55.
10. Mazurenko NN, Kogan EA, Zborovskaya IB, Kisseljov FL. Expression of pp60c-src in human small cell and non-small cell lung carcinomas. Eur J Cancer 1992;28:372–7.
11. Laird AD, Li G, Moss KG, et al. Src family kinase activity is required for signal tranducer and activator of transcription 3 and focal adhesion kinase phosphorylation and vascular endothelial growth factor signaling *in vivo* and for anchorage-dependent and -independent growth of human tumor cells. Mol Cancer Ther 2003;2:461–9.
12. Song L, Turkson J, Karras JG, Jove R, Haura EB. Activation of Stat3 by receptor tyrosine kinases and cytokines regulates survival in human non-small cell carcinoma cells. Oncogene 2003;22:4150–65.
13. van Oijen MG, Rijksen G, ten Broek FW, Slootweg PJ. Overexpression of c-Src in areas of hyperproliferation in head and neck cancer, premalignant lesions and benign mucosal disorders. J Oral Pathol Med 1998;27:147–52.
14. Bu R, Purushotham KR, Kerr M, et al. Alterations in the level of phosphotyrosine signal transduction constituents in human parotid tumors. Proc Soc Exp Biol Med 1996;211:257–64.
15. Xi S, Zhang Q, Dyer KF, et al. Src kinases mediate STAT growth pathways in squamous cell carcinoma of the head and neck. J Biol Chem 2003;278:31574–83.
16. Lombardo LJ, Lee FY, Chen P, et al. Discovery of *N*-(2-chloro-6-methyl-phenyl)-2-(6-(4-(2-hydroxyethyl)-piperazin-1-yl)-2-methylpyrimidin-4-ylamino)thiazole-5-carboxamide (BMS-354825), a dual Src/Abl kinase inhibitor with potent antitumor activity in preclinical assays. J Med Chem 2004;47:6658–61.
17. Shah NP, Tran C, Lee FY, Chen P, Norris D, Sawyers CL. Overriding imatinib resistance with a novel ABL kinase inhibitor. Science 2004;305:399–401.
18. Burgess MR, Skaggs BJ, Shah NP, Lee FY, Sawyers CL. Comparative analysis of two clinically active BCR-ABL kinase inhibitors reveals the role of conformation-specific binding in resistance. Proc Natl Acad Sci U S A 2005;102:3395–400.
19. Donato NJ, Perez M. Tumor necrosis factor-induced apoptosis stimulates p53 accumulation and p21WAF1 proteolysis in ME-180 cells. J Biol Chem 1998;273:5067–72.
20. Mujoo K, Maneval DC, Anderson SC, Gutterman JU. Adenoviral-mediated *p53* tumor suppressor gene therapy of human ovarian carcinoma. Oncogene 1996;12:1617–23.
21. Kong-Beltran M, Stamos J, Wickramasinghe D. The Sema domain of Met is necessary for receptor dimerization and activation. Cancer Cell 2004;6:75–84.

22. Michieli P, Mazzone M, Basilico C, et al. Targeting the tumor and its microenvironment by a dual-function decoy Met receptor. Cancer Cell 2004;6:61–73.

23. Albini A, Iwamoto Y, Kleinman HK, et al. A rapid *in vitro* assay for quantitating the invasive potential of tumor cells. Cancer Res 1987;47:3239–45.

24. Talpaz M, Kantarjian H, Shah NP, et al. Hematologic and cytogenetic responses in imatinib-resistant accelerated and blast phase chronic myeloid leukemia (CML) patients treated with the dual SRC/ABL kinase inhibitor BMS-354825: results from a phase I dose escalation study. Blood 2004;104:20.

25. Sawyers C, Shah NP, Kantarjian H, et al. Hematologic and cytogenetic responses in imatinib-resistant chronic phase chronic myeloid leukemia patients treated with the dual SRC/ABL kinase inhibitor BMS-354825: results from a phase I dose escalation study. Blood 2004;104:1.

26. Jokinen J, Dadu E, Nykvist P, et al. Integrin-mediated cell adhesion to type I collagen fibrils. J Biol Chem 2004;279:31956–63.

27. Farrelly N, Lee YJ, Oliver J, Dive C, Streuli CH. Extracellular matrix regulates apoptosis in mammary epithelium through a control on insulin signaling. J Cell Biol 1999;144:1337–48.

28. Massague J. G_1 cell-cycle control and cancer. Nature 2004;432:298–306.

29. Abram CL, Courtneidge SA. Src family tyrosine kinases and growth factor signaling. Exp Cell Res 2000;254:1–13.

30. Olayioye MA, Badache A, Daly JM, Hynes NE. An essential role for Src kinase in ErbB receptor signaling through the MAPK pathway. Exp Cell Res 2001;267:81–7.

31. Wakeling AE, Guy SP, Woodburn JR, et al. ZD1839 (Iressa): an orally active inhibitor of epidermal growth factor signaling with potential for cancer therapy. Cancer Res 2002;62:5749–54.

32. Janmaat ML, Kruyt FA, Rodriguez JA, Giaccone G. Response to epidermal growth factor receptor inhibitors in non-small cell lung cancer cells: limited antiproliferative effects and absence of apoptosis associated with persistent activity of extracellular signal-regulated kinase or Akt kinase pathways. Clin Cancer Res 2003;9:2316–26.

33. Lynch TJ, Bell DW, Sordella R, et al. Activating mutations in the epidermal growth factor receptor underlying responsiveness of non-small-cell lung cancer to gefitinib. N Engl J Med 2004;350:2129–39.

34. Paez JG, Janne PA, Lee JC, et al. EGFR mutations in lung cancer: correlation with clinical response to gefitinib therapy. Science 2004;304:1497–500.

35. Raben D, Helfrich B, Chan DC, et al. The effects of cetuximab alone and in combination with radiation and/or chemotherapy in lung cancer. Clin Cancer Res 2005;11:795–805.

36. Kalyankrishna S, Zhang J, Johnson FM, Kurie JM. Ligand-independent activation of mutant EGFR in lung cancer cells: enhanced sensitivity to c-Src tyrosine kinase inhibitors. Anaheim (CA): American Association for Cancer Research; 2005. Abstract 4316.

37. Rengifo-Cam W, Konishi A, Morishita N, et al. Csk defines the ability of integrin-mediated cell adhesion and migration in human colon cancer cells: implication for a potential role in cancer metastasis. Oncogene 2004;23:289–97.

38. Patarroyo M, Tryggvason K, Virtanen I. Laminin isoforms in tumor invasion, angiogenesis and metastasis. Semin Cancer Biol 2002;12:197–207.

39. Velling T, Nilsson S, Stefansson A, Johansson S. β1-integrins induce phosphorylation of Akt on serine 473 independently of focal adhesion kinase and Src family kinases. EMBO Rep 2004;5:901–5.

40. Johnson FM, Saigal B, Donato NJ. Induction of heparin-binding EGF-like growth factor and activation of EGF receptor in imatinib mesylate-treated squamous carcinoma cells. J Cell Physiol. In press 2005.

41. Johnson FM, Yang P, Newman RA, Donato NJ. Cyclooxygenase-2 induction and prostaglandin E_2 accumulation in squamous cell carcinoma as a consequence of epidermal growth factor receptor activation by imatinib mesylate. J Exp Ther Oncol 2004;4:317–25.

42. Kinch MS, Moore MB, Harpole DH, Jr. Predictive value of the EphA2 receptor tyrosine kinase in lung cancer recurrence and survival. Clin Cancer Res 2003;9:613–8.

43. Gray MJ, Zhang J, Ellis LM, et al. HIF-1α, STAT3, CBP/p300 and Ref-1/APE are components of a transcriptional complex that regulates Src-dependent hypoxia-induced expression of VEGF in pancreatic and prostate carcinomas. Oncogene 2005;24:3110–20.